Acta Cryst. (1979). B**35**, 1303–1308

Electron-Density Distribution in Crystals of $KCuF_3$ with Jahn–Teller Distortion

BY K. TANAKA, M. KONISHI AND F. MARUMO

The Research Laboratory of Engineering Materials, Tokyo Institute of Technology, O-okayama 2-12-1, *Meguro-ku, Tokyo* 152, *Japan*

(*Received* 1 *November* 1978; *accepted* 7 *February* 1979)

Abstract

The electron-density distribution in crystals of $K^+[CuF_3]^-$ has been investigated on the basis of X-ray intensity data collected by diffractometry at room temperature. The crystal has a distorted perovskite structure, containing Cu^{2+} ions at pseudo-tetragonally deformed octahedral sites. On the deformation-density map, positive peaks were observed on the longest Cu–F bonds and negative peaks on the shortest Cu–F near the Cu^{2+} ion. When aspherical scattering factors were used for Cu^{2+} by assuming the hole of the *d* shell on the $d_{x^2-y^2}$ orbital, the difference Fourier map showed large positive peaks on the Cu–F bonds with intermediate length, though the positive and negative peaks on the longest and shortest bonds disappeared. The observed electron density is well explained if we assume that the hole occupies the orbital given by $\sin(\varphi/2)d_{z^2} - \cos(\varphi/2)d_{x^2-y^2}$. The most plausible value of $\cos(\varphi/2)$ after the least-squares fit was 0·976 (17). The experimental density distribution of the 3*d* electrons in the $3d_\gamma$ orbitals was obtained, revealing well the origin of the deformation-density maps.

Introduction

Recently, spatial distributions of *d* electrons have been investigated in several crystals of transition-metal compounds, *e.g.* $[Co(NH_3)_6][Co(CN)_6]$ (Iwata & Saito, 1973), γ-Ni_2SiO_4 (Marumo, Isobe, Saito, Yagi & Akimoto, 1974), γ-Fe_2SiO_4 and γ-Co_2SiO_4 (Marumo, Isobe & Akimoto, 1977), $(+)_{589}$-$[Rh(R,R\text{-chxn})_3](NO_3)_3.3H_2O$ (Miyamae, Sato & Saito, 1977), $CoAl_2O_4$ (Toriumi, Ozima, Akaogi & Saito, 1978), *etc.* In all cases, peaks indicating deformation from spherical distributions have been observed on the difference Fourier maps. Johansen (1976) theoretically treated three transition-metal complexes, $Ni(CH_3)_2$, MnO_4^- and CoO_6^{10-}, and showed that pronounced deformation peaks appear around the metal atoms at spaces avoiding the ligands. This feature coincides qualitatively with the experimental results, although the peaks are too high and too close to the centres of the atoms compared with the experiments. The discrepancy was attributed to the ambiguity of the thermal factors in the theory.

$KCuF_3$ was selected for the further study of 3*d* electron-density distribution by the X-ray diffraction method. The crystal suits this purpose since the structure is simple and extensive studies have been carried out on the electronic state. Crystals of $KCuF_3$ have distorted perovskite structures and two modifications, type *a* and type *b*, are known (Okazaki, 1969*a*,*b*). Type *a* crystals are more common, having the stacking shown in Fig. 1 (Okazaki & Suemune, 1961). In this structure the F(2) atom at an 8(*h*) position of the space group $I4/mcm$ is displaced from the midpoint between two neighbouring Cu atoms in the (001) plane, forming a short and a long Cu–F bond. The Cu–F(1) distance lies between the two Cu–F(2) distances, but it is much closer to the shorter one. Accordingly, the coordination octahedron of the Cu atom has pseudo-tetragonal symmetry. In the following discussion, we denote the F atom at the longest, intermediate and shortest distances from a central Cu atom as F_l, F_m and F_s, respectively. The distortion is attributed to a cooperative Jahn–Teller effect (Kanamori, 1960), and the directions of the displacements of the F(2) atoms alternate along the *c* axis, doubling the *c* period of the cubic perovskite structure.

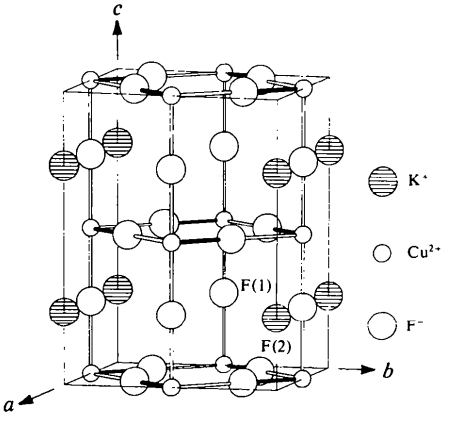

Fig. 1. Crystal structure of $KCuF_3$ (type *a*). Bold lines indicate short Cu–F_s bonds. The unit cell is shown by fine single lines.

0567-7408/79/061303-06$01.00

A refinement of the structure was recently performed by Tanaka, Konishi & Marumo (1977) and large negative peaks were found around the Cu atom on the final difference Fourier map, which seemed to indicate the distribution of the hole on the Cu^{2+} ion in an octahedral field distorted by the Jahn–Teller effect.

In the present study, much improved maps of deformation density were obtained and the analysis was carried out with aspherical scattering factors for the Cu^{2+} ion.

Experimental

A crystal was cut from a large block of $KCuF_3$ polycrystals synthesized by Ikeda & Hirakawa (1973) for their neutron diffraction studies. It was shaped into a sphere of 0·11 mm diameter, by gently rubbing it on a piece of filter paper wetted with dilute nitric acid, to ensure constant illumination of X-rays on the specimen (Tanaka, 1978) and to facilitate the intensity corrections. From oscillation and Weissenberg photographs the crystal was ascertained to be the type *a* modification of Okazaki (1969*a*,*b*).

The cell dimensions were determined from 72 2θ values measured on a four-circle diffractometer with Mo $K\alpha$ radiation in the range higher than 94°, where $K\alpha_1$ and $K\alpha_2$ were clearly separated. They are given in Table 1 together with other crystal data.

Intensities of reflexions in an octant of the reciprocal space were collected on a Rigaku automated four-circle diffractometer with graphite-monochromated Mo $K\alpha$ radiation. The ratio of the counting time of the background to the scan time of a peak was varied for each reflexion in proportion to the square root of the ratio between their mean counting rates (after Shoemaker, 1968). To avoid counting loss, a nickel-foil attenuator of appropriate thickness was automatically inserted when the diffracted-beam intensity exceeded 5000 counts s^{-1}. Each reflexion was repeatedly measured (up to eight times) to reduce the statistical counting error of the structure factor. Experimental conditions are summarized in Table 2.

Corrections for the Lp factors were performed. Absorption was corrected for with the values of the absorption-correction factors, A^*, tabulated in *International Tables for X-ray Crystallography* (1967). The mean path length $\bar{T} = (dA^*/d\mu)/A^*$ was calculated for each reflexion in view of the extinction correction. Here, μ is the linear absorption coefficient, and $dA^*/d\mu$ was obtained by numerical differentiation. Weak reflexions with $|F| < 3\sigma(|F|)$ were excluded from the data set, where $\sigma(|F|)$ is the standard deviation of the observed structure amplitude due to counting statistics.

Table 1. *Crystal data of* $KCuF_3$ *at* 296 K

Tetragonal $I4/mcm$	
$a = 5{\cdot}8633\ (5)$ Å	$Z = 4$
$c = 7{\cdot}8470\ (6)$	$D_x = 3{\cdot}937$ Mg m^{-3}
$V = 269{\cdot}77\ (6)$ Å^3	μ(Mo $K\alpha$) = 9·743 mm^{-1}

Table 2. *Experimental conditions*

Diameter of the specimen	0·11 mm
Radiation	Mo $K\alpha$
Monochromator	Graphite
$2\theta_{max}$ of the observed reflexion	140°
Scan technique	ω–2θ
Scan speed	4° min^{-1} in 2θ
Scan width	$(1{\cdot}2 + 1{\cdot}0 \tan\theta)°$
Maximum number of repetitions	8
Criterion to terminate repetition	$\sigma(\|F\|)/\|F\| = 0{\cdot}0025$
Number of reflexions measured	989
Number of reflexions used	959

Refinement

Four kinds of least-squares refinements were carried out by changing the electron configuration model for the Cu^{2+} ion in the calculation of the atomic scattering factors. For the first step, the usual spherical scattering factors of free ions were employed for all the constituent atoms. In the second, aspherical scattering factors were used for the Cu^{2+} ion, assuming that the ion was placed in an ideally tetragonal ligand field. In the third refinement, the distortion of the ligand field to an orthorhombic symmetry was taken into account, and finally a 'double-atom' refinement was tried by dividing the Cu^{2+} ion into the Ar core and nine 3*d* electrons in the outer shell. The atomic and extinction parameters obtained in these four refinements are tabulated in columns (*a*), (*b*), (*c*) and (*d*) of Table 3, respectively.

(*a*) *Refinement with the spherical scattering factors*

The atomic parameters reported by Okazaki & Suemune (1961) were used for the starting values of the full-matrix least-squares refinement. Atomic scattering and dispersion-correction factors were taken from *International Tables for X-ray Crystallography* (1974) for Cu^{2+}, K^+ and F^- ions. In this structure, the positional parameter to be determined is only the x coordinate of F(2) at the 8(*h*) position. The refinement was carried out with the modified version of *LINEX* including the extinction correction after Becker & Coppens (1974*a*,*b*, 1975). After the refinement without the extinction correction, $R_1 = \sum(||F_o| - |F_c||)/\sum|F_o|$ and $R_2 = [\sum(|F_o| - |F_c|)^2/\sum|F_o|^2]^{1/2}$ were 0·062 and 0·091, respectively. Since there was a large deviation between the observed and calculated structure factors of the 220 reflexion (F_o = 145·75, F_c = 198·72), it was excluded in all the subsequent refinements. The refinement

with an extinction correction of the anisotropic type I, based on the assumption of the Gaussian mosaic spread distribution, gave much better R values (0·014 for both R_1 and R_2) than that with the extinction correction of type II.

(*b*) *Refinement assuming a hole on the* $3d_{x^2-y^2}$ *orbital*

As described above, the Cu^{2+} ion is placed in an approximately tetragonal field in this structure. In an ideal tetragonal field, the fivefold-degenerate $3d$ orbitals split into four levels, that is, a doubly-degenerate orbital composed of d_{xz} and d_{yz}, and three non-degenerate orbitals, d_{xy}, d_{z^2} and $d_{x^2-y^2}$. All these orbitals are filled with pairs of electrons except the half-filled $d_{x^2-y^2}$ orbital in the ground state of a Cu^{2+} ion placed in a tetragonal field. Refinement was carried out on this electron-configuration model, taking the quantization axis z along the Cu–F_l bond.

The scattering factor for each of the five $3d$ orbitals is expressed in the form,

$$f_{3d} = \langle j_0 \rangle + A(3\cos^2\beta - 1)\langle j_2 \rangle + B(\cos\beta \sin^2\beta \cos 2\gamma)\langle j_2 \rangle + C(35\cos^4\beta - 30\cos^2\beta + 3)\langle j_4 \rangle + D\sin^2\beta(7\cos^2\beta - 1)\cos 2\gamma \langle j_4 \rangle + E\sin^4\beta \cos 4\gamma \langle j_4 \rangle,$$

where the coefficients, A, B, C, D and E, depend on the sort of $3d$ orbital, as given in Table 4; the values of the $\langle j_n \rangle$'s are tabulated in *International Tables for X-ray Crystallography* (1974); β and γ are the angular coordinates of the scattering vector (Weiss & Freeman, 1959; Iwata, 1977). The least-squares calculations were performed with *LINKT* written by one of the authors (KT). The R_1 and R_2 values reduced only slightly to 0·0139.

(*c*) *Refinement assuming an orthorhombic Jahn–Teller distortion*

A small but significant difference exists between the lengths of the Cu–F_m and Cu–F_s bonds. The distortion is ascribed to a cooperative Jahn–Teller effect, and it is necessary to consider the linear combination of d_{z^2} and $d_{x^2-y^2}$ orbitals to express the electronic state,

$$\Psi_g = \cos(\varphi/2)d_{z^2} + \sin(\varphi/2)d_{x^2-y^2},$$
$$\Psi_e = \sin(\varphi/2)d_{z^2} - \cos(\varphi/2)d_{x^2-y^2}.$$

Ψ_g and Ψ_e are assumed to be doubly and singly occupied, respectively. The scattering factors for these orbitals are:

$$f_g = \cos^2(\varphi/2)f_{z^2} + \sin^2(\varphi/2)f_{x^2-y^2} + \sin\varphi f_{z^2,x^2-y^2},$$
$$f_e = \sin^2(\varphi/2)f_{z^2} + \cos^2(\varphi/2)f_{x^2-y^2} - \sin\varphi f_{z^2,x^2-y^2},$$

where f_{z^2}, $f_{x^2-y^2}$ and f_{z^2,x^2-y^2} are the scattering factors for the $3d_{z^2}$ and $3d_{x^2-y^2}$ orbitals and for the orbital product of $3d_{z^2}$ and $3d_{x^2-y^2}$, respectively. The explicit form of f_{z^2,x^2-y^2} is

$$f_{z^2,x^2-y^2} = [(5\sqrt{3}/7)\sin^2\beta\langle j_2 \rangle + (15\sqrt{3}/28)\sin^2\beta(7\cos^2\beta - 1)\langle j_4 \rangle]\cos 2\gamma.$$

The x, y and z axes were taken along the Cu–F_s, Cu–F_m and Cu–F_l bonds, respectively. Least-squares calculations were performed by adding $\cos(\varphi/2)$ to the parameters to be refined. The refinement reduced significantly both the R_1 and R_2 factors to 0·0128, giving the value 0·964 (18) for $\cos(\varphi/2)$.

Table 3. *The positional parameters* ($\times 10^5$), *anisotropic temperature factors* ($\times 10^5$ Å^{-2}), *anisotropic extinction parameters* ($\times 10^3$) *and the coefficient* $\cos(\varphi/2)$ ($\times 10^3$)

The atomic positions are (0,½,0) for Cu, (0,0,¼) for K, (0,½,¼) for F(1) and (x, x + ½, 0) for F(2). The form of the anisotropic temperature factor is defined as $\exp\{-2\pi^2[(h^2 + k^2)a^{*2}U_{11} + l^2c^{*2}U_{33} + 2hka^*b^*U_{12}]\}$.

Type of refinement		(*a*)	(*b*)	(*c*)	(*d*)
Cu	U_{11}	753 (3)	745 (3)	758 (3)	761 (3)*
	U_{33}	583 (4)	594 (4)	570 (4)	579 (3)*
	U_{12}	−139 (4)	−107 (4)	−94 (4)	−94 (4)*
K	U_{11}	1534 (6)	1534 (6)	1533 (5)	1539 (5)
	U_{33}	1438 (8)	1435 (8)	1438 (7)	1445 (7)
F(1)	U_{11}	2226 (21)	2203 (20)	2223 (19)	2231 (19)
	U_{33}	716 (18)	724 (18)	714 (16)	718 (16)
F(2)	x	22762 (7)	22768 (7)	22768 (6)	22769 (6)
	U_{11}	1357 (12)	1350 (12)	1352 (11)	1359 (11)
	U_{33}	1954 (22)	1961 (22)	1953 (20)	1956 (20)
	U_{12}	−635 (16)	−639 (16)	−638 (15)	−641 (14)
3*d*	U_{11}				797 (56)†
	U_{33}				836 (75)†
	U_{12}				−133 (56)†
$\cos(\varphi/2)$				964 (18)	976 (17)
G_{11}		76 (4)	76 (4)	78 (3)	82 (3)
G_{22}		133 (5)	136 (5)	135 (5)	136 (5)
G_{33}		267 (36)	304 (37)	286 (34)	267 (33)
G_{12}		66 (2)	67 (2)	69 (2)	71 (2)
G_{13}		−64 (9)	−66 (9)	−63 (9)	−58 (9)
G_{23}		−28 (16)	−32 (17)	−25 (15)	−13 (15)

* Temperature factors for the Ar core in the refinement (*d*).
† Temperature factors for the 3*d* electrons in the refinement (*d*).

Table 4. *Coefficients of the aspherical scattering factors of the* 3*d electrons*

	A	*B*	*C*	*D*	*E*
d_{xy}	$\frac{5}{7}$		$\frac{3}{56}$		$-\frac{15}{8}$
d_{xz}	$-\frac{5}{14}$	$\frac{15}{14}\sqrt{7}$	$-\frac{3}{14}$	$\frac{15}{14}$	
d_{yz}	$-\frac{5}{14}$	$-\frac{15}{14}\sqrt{7}$	$-\frac{3}{14}$	$-\frac{15}{14}$	
$d_{x^2-y^2}$	$\frac{5}{7}$		$\frac{3}{56}$		$\frac{15}{8}$
d_{z^2}	$-\frac{5}{7}$		$\frac{9}{28}$		

(d) Double-atom refinement

Since the $3d$ electrons of the Cu^{2+} ion interact strongly with the ligands, the thermal motions of these electrons might be different from that of the Ar core. Therefore, the 'double-atom' refinement was tried by dividing the Cu^{2+} ion into two parts, the Ar core and the outer-shell $3d$ electrons. The temperature factors of the $3d$ electrons and cos $(\varphi/2)$ were refined alternately because of their large correlation. The value 0·976 (17) was obtained for cos $(\varphi/2)$, and R_1 and R_2 reduced only slightly to 0·0127.*

Results and discussion

The Cu–F_s, Cu–F_m and Cu–F_l bond lengths calculated with the final x value of F(2) in the double-atom refinement are 1·8880 (5), 1·9618 (2) and 2·2580 (5) Å, respectively. All the refinements gave the same values within experimental error.

Fig. 2 shows the deformation density around the Cu^{2+} ion obtained after the spherical-atom refinement. A large negative peak with a depth of $-1·57$ e Å^{-3} is observed on the Cu–F_s bond at 0·52 Å from the Cu^{2+} ion, while a positive peak with height 0·57 e Å^{-3} exists on the Cu–F_l bond at 0·62 Å from the central cation. On the Cu–F_m bond only a small negative peak is observed near the Cu^{2+} ion. These features roughly agree with the electron-configuration model, in which a hole is allotted to the $3d_{x^2-y^2}$ orbital spreading along the Cu–F_s and Cu–F_m bonds. Actually, the negative and positive peaks on the Cu–F_s and Cu–F_l bonds were reduced in magnitude to $-0·73$ and 0·32 e Å^{-3}, respectively, in the difference Fourier map synthesized with the parameters obtained in the refinement assuming a hole on the $3d_{x^2-y^2}$ orbital, as shown in Fig. 3. On the other hand, a new positive peak with a height of 1·17 e Å^{-3} appeared on Cu–F_m as expected from the difference between the residual densities of the Cu–F_s and Cu–F_m bonds in the deformation density map. The peak is 0·47 Å from the Cu^{2+} ion. The difference between the electron densities on Cu–F_s and Cu–F_m is in conformity with the difference between the bond lengths, and suggests that it is necessary to use orbitals made up of the linear combinations of $3d_{z^2}$ and $3d_{x^2-y^2}$ to obtain a better fitting to the observed electron distribution. Therefore, refinement was carried out utilizing the orbitals Ψ_g and Ψ_e as already stated. The difference Fourier map synthesized after the refinement is shown in Fig. 4. The large positive and negative peaks on Cu–F_m and Cu–F_s in Fig. 3 completely disappeared and, as a whole, a better agreement was obtained between experimental and postulated electron distributions than in Fig. 3, although several new peaks grew up around the Cu^{2+} ion. The better agreement of the electron distributions, as well as the small R values, suggests that the deformation of the densities around the Cu^{2+} ion is actually caused by the Jahn–Teller effect.

* Lists of structure factors and anisotropic thermal parameters have been deposited with the British Library Lending Division as Supplementary Publication No. SUP 34261 (9 pp.). Copies may be obtained through The Executive Secretary, International Union of Crystallography, 5 Abbey Square, Chester CH1 2HU, England.

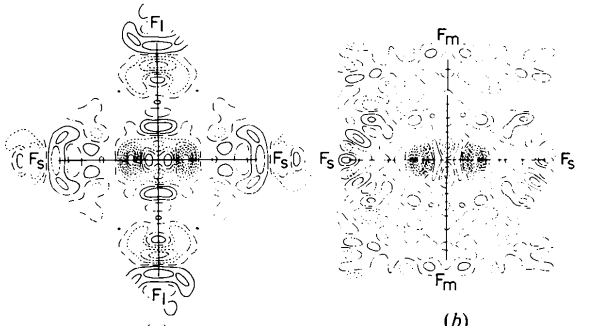

Fig. 2. The sections of the difference Fourier map after the refinement with the spherical scattering factors through the planes determined (*a*) by the Cu–F_s and Cu–F_l bonds, (*b*) by the Cu–F_s and Cu–F_m bonds. Contours are at intervals of 0·2 e Å^{-3}. Negative and zero contours are in broken and dashed–dotted lines, respectively.

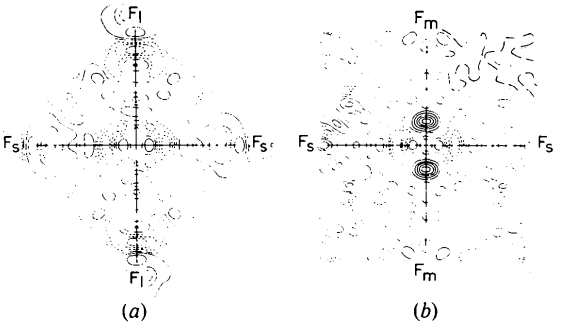

Fig. 3. The sections of the difference Fourier map after the refinement assuming a hole on the $3d_{x^2-y^2}$ orbital through the same planes as in Fig. 2. Contours are at intervals of 0·2 e Å^{-3}. Negative and zero contours are in broken and dashed–dotted lines, respectively.

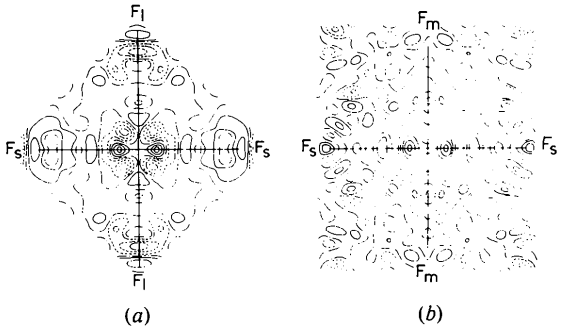

Fig. 4. The sections of the difference Fourier map after the refinement assuming an orthorhombic Jahn–Teller distortion, through the same planes as in Fig. 2. Contours are at intervals of 0·2 e Å^{-3}. Negative and zero contours are in broken and dashed–dotted lines, respectively.

A difference Fourier map was also synthesized after the double-atom refinement (Fig. 5). The positive and negative peaks around the Cu^{2+} ion were reduced from 0·67 and −0·79 e Å^{-3} to 0·51 and −0·63 e Å^{-3}, respectively, and the peaks became smoother than those in Fig. 4, indicating the better fit of the curves of the calculated electron density to those of the observed one. These minor peaks are due to some effects or errors which were not taken into account. Non-localized electrons of the F^- ion were not considered and the thermal factors were determined assuming harmonic vibration of atoms.

The experimental density distribution of $3d$ electrons on the $3d_\gamma$ orbitals was obtained by synthesizing the difference Fourier function with coefficients $F_o - F_{c,\gamma}$, where $F_{c,\gamma}$ are the structure factors calculated excluding the contribution of the $3d_\gamma$ electrons on the Ψ_g and Ψ_e orbitals. The result is shown in Fig. 6. The electron density is markedly elongated along the Cu–F_l and Cu–F_m bonds compared with the direction along Cu–F_s. Thus, the map reveals the origin of the deformation density in Fig. 2.

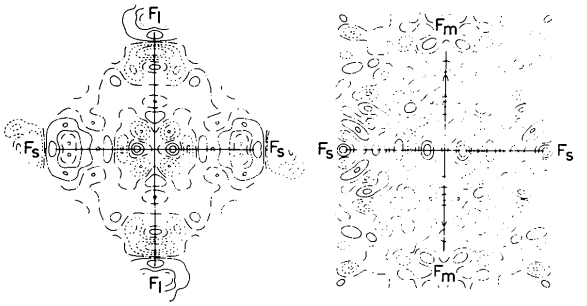

Fig. 5. The sections of the difference Fourier map after the double-atom refinement through the same planes as in Fig. 2. Contours are at intervals of 0·2 e Å^{-3}. Negative and zero contours are in broken and dashed–dotted lines, respectively.

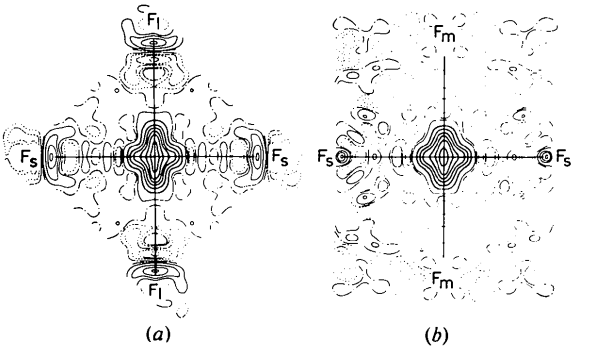

Fig. 6. The experimental density distribution of $3d$ electrons on the Ψ_g and Ψ_e orbitals, through the same planes as in Fig. 2. Contours in thin and thick lines are at intervals of 0·2 and 1·0 e Å^{-3}, respectively. Negative and zero contours are in broken and dashed–dotted lines, respectively.

Kadota, Yamada, Yoneyama & Hirakawa (1967) determined the coefficient cos $(\varphi/2)$ to be 0·816 from the differences between the Cu–F bond lengths, taking the x, y and z axes along the Cu–F_s, Cu–F_l and Cu–F_m bonds, respectively. The value is transformed to 0·908 in our coordinate system, and is significantly smaller than 0·976 obtained in the present study.

The F^- ion has a closed-shell electron configuration. However, Figs. 2 to 6 reveal that the electron density is higher on the Cu–F_s bond than on the Cu–F_l. This may imply that the electrons around the F^- ion are attracted towards the closer Cu^{2+} ion.

In an ordinary least-squares refinement there is always the possibility of incorporating a part of the asphericity of the electron density distribution into the asphericity of the thermal motion (McWeeny, 1951). Therefore, it is interesting to follow the change of the temperature factors of the Cu^{2+} ion through the refinement processes. The r.m.s. displacements along the three principal axes of the thermal ellipsoid are given by $(U_{11} + U_{12})^{1/2}$, $(U_{11} - U_{12})^{1/2}$ and $U_{33}^{1/2}$, since these axes are restricted by the symmetry to lie along the Cu–F_s, Cu–F_l and Cu–F_m bonds, respectively. As seen in Table 3, only the Cu^{2+} ion showed significant changes of temperature factor due to the difference of the electron-configuration model in the refinement procedure. Among the three thermal parameters of the Cu^{2+} ion, U_{33} showed the smallest dependence on the type of scattering factor. U_{11} and U_{12} changed in such a way that more isotropic temperature factors resulted when the asphericity of the $3d$ electron distribution was taken more exactly into account. The temperature factors of the Ar core in the double-atom refinement are close to those of the Cu^{2+} ion in the preceding refinement, while the outer-shell $3d$ electrons have much larger temperature factors than the Ar core. This may be partly due to an expansion of the $3d$ orbitals in the ligand field.

The authors wish to express their gratitude to Professor Y. Saito of the Institute for Solid State Physics, The University of Tokyo, for providing facilities to collect intensity data. They are grateful to Professor H. Ikeda of Ochanomizu University for kindly supplying the crystal specimen, and to Professor P. Coppens for sending a copy of the program *LINEX*. They also wish to express their thanks to Professors H. Hirakawa of the Institute for Solid State Physics and H. Kobayashi of the Tokyo Institute of Technology for their kind advice and valuable discussions. Fig. 1 was drawn with the Fortran program *DCMS* written by Dr A. Takenaka of the Tokyo Institute of Technology, to whom the authors' thanks are due. Part of the cost of this research was met by a Scientific Research Grant from the Ministry of Education, to which the authors' thanks are due.

References

BECKER, P. J. & COPPENS, P. (1974*a*). *Acta Cryst.* A**30**, 129–147.

BECKER, P. J. & COPPENS, P. (1974*b*). *Acta Cryst.* A**30**, 148–153.

BECKER, P. J. & COPPENS, P. (1975). *Acta Cryst.* A**31**, 417–425.

IKEDA H. & HIRAKAWA, K. (1973). *J. Phys. Soc. Jpn*, **35**, 722–728.

International Tables for X-ray Crystallography (1967). Vol. II. Birmingham: Kynoch Press.

International Tables for X-ray Crystallography (1974). Vol. IV. Birmingham: Kynoch Press.

IWATA, M. (1977). *Acta Cryst.* B**33**, 59–69.

IWATA, M. & SAITO, Y. (1973). *Acta Cryst.* B**29**, 822–832.

JOHANSEN, H. (1976). *Acta Cryst.* A**32**, 353–355.

KADOTA, S., YAMADA, I., YONEYAMA, S. & HIRAKAWA, K. (1967). *J. Phys. Soc. Jpn*, **23**, 751–756.

KANAMORI, J. (1960), *J. Appl. Phys.* **31**, suppl. 14S–23S.

MCWEENY, R. (1951). *Acta Cryst.* **4**, 513–519.

MARUMO, F., ISOBE, M. & AKIMOTO, S. (1977). *Acta Cryst.* B**33**, 713–716.

MARUMO, F., ISOBE, M., SAITO, Y., YAGI, T. & AKIMOTO, S. (1974). *Acta Cryst.* B**30**, 1904–1906.

MIYAMAE, H., SATO, S. & SAITO, Y. (1977). *Acta Cryst.* B**33**, 3391–3396.

OKAZAKI, A. (1969*a*). *J. Phys. Soc. Jpn*,**26**, 870.

OKAZAKI, A. (1969*b*). *J. Phys. Soc. Jpn*,**27**, 518.

OKAZAKI, A. & SUEMUNE, Y. (1961). *J. Phys. Soc. Jpn*, **16**, 176–183.

SHOEMAKER, D. P. (1968). *Acta Cryst.* A**24**, 136–142.

TANAKA, K. (1978). *Acta Cryst.* B**34**, 2487–2492.

TANAKA, K., KONISHI, M. & MARUMO, F. (1977). *Rep. Res. Lab. Eng. Mater., Tokyo Inst. Technol.* **3**, 19–26.

TORIUMI, K., OZIMA, M., AKAOGI, M. & SAITO, Y. (1978). *Acta Cryst.* B**34**, 1093–1096.

WEISS, R. J. & FREEMAN, A. J. (1959). *J. Phys. Chem. Solids*, **10**, 147–161.

Acta Cryst. (1979). B**35**, 1308–1312

Crystal Structure of $K_3N(SO_3)_2.H_2O$ (I) and Refinement of the Crystal Structure of $K_2NH(SO_3)_2$ (II)

BY PIERRE BARBIER, YVES PARENT AND GAËTAN MAIRESSE

Laboratoire de Chimie Minérale I, *Université des Sciences et Techniques de Lille, BP* 36, 59 650 *Villeneuve d'Ascq, France*

(*Received* 30 *December* 1978; *accepted* 12 *February* 1979)

Abstract

Crystal (I) is triclinic, space group $P\bar{1}$, with a = 8·126 (4), b = 7·978 (3), c = 6·762 (4) Å, α = 103·36 (3), β = 90·98 (3), γ = 97·86 (3)°, Z = 2. The structure was refined to R = 0·029 for 2067 reflexions. The bond lengths are S—N = 1·606 and S—O = 1·468 Å, and bond angles are S—N—S = 120·83 (11) and N—S—O = 108·70°. The structure of (II) has been refined to a final R = 0·043 over 1113 reflexions. The H atom was observed, and its coordinates agree well with those obtained earlier by neutron diffraction.

Introduction

Studies of various S- and N-containing compounds, *e.g.* SO_3NH_3, $[SO_3NH_2]^-$, $[(SO_3)_2NH]^{2-}$, have shown that S—O and S—N lengths vary over a wide range. Cruickshank (1961) explained the contraction of the S—O and S—N bonds by the formation of two strong π-bonding molecular orbitals. The formation of such orbitals is possible only if there are p orbitals available for the π systems on the bridge atom.

Thus, if the bridge atom (N) in $K_3N(SO_3)_2$ is replaced by NH in $K_2NH(SO_3)_2$, we should observe S—O and S—N bond-length variations, since the number of p orbitals available on the N atom is different in the two compounds.

For this reason we have undertaken the X-ray structural analysis of the two compounds. The crystal structure of $K_3N(SO_3)_2.H_2O$ is unknown, but that of $K_2NH(SO_3)_2$ has been determined by X-ray diffraction (Jeffrey & Jones, 1956). Further refinement of the data was made by Cruickshank & Jones (1963). More recently, Hodgson, Moore & Kennard (1976) redetermined the structure by neutron diffraction. They showed that the N atom is surrounded tetrahedrally by two SO_3 groups and two half H atoms. As crystals of good quality were available, we have refined the structure of this salt, and determined that of $K_3N(SO_3)_2.H_2O$.

0567-7408/79/061308-05$01.00